Hydrogen adsorption on boron doped graphene: an *ab initio* study

R. H. Miwa[1], T. B. Martins[2], and A. Fazzio[2]
[1] *Instituto de Física, Universidade Federal de Uberlândia, Caixa Postal 593, 38400-902, Uberlândia, MG, Brazil. and*
[2] *Instituto de Física, Universidade de São Paulo, Caixa Postal 66318, 05315-970, São Paulo, SP, Brazil.*

(Dated: February 1, 2008)

The electronic and structural properties of (i) boron doped graphene sheets, and (ii) the chemisorption processes of hydrogen adatoms on the boron doped graphene sheets have been examined by *ab initio* total energy calculations. In (i) we find that the structural deformations are very localized around the boron substitutional sites, and there is an increase of the electronic density of states near the Fermi level. Our simulated STM images, for occupied states, indicate the formation of a bright (triangular) spots lying on the substitutional boron (center) and nearest neighbor carbon (edge) sites. Those STM pictures are attributed to the increase of the density of states within an energy interval of 0.5 eV below the Fermi level. For boron concentration of $\sim$2.4%, we find that two boron atoms lying on the opposite sites of the same hexagonal ring ($B1$-$B2$ configuration) represents the energetically most stable configuration, which is in contrast with previous theoretical findings. Having determined the energetically most stable configuration for substitutional boron atoms on graphene sheets, we next considered the hydrogen adsorption process as a function of the boron concentration, (ii). Our calculated binding energies indicate that the C–H bonds are strengthened nearby boron substitutional sites. Indeed, the binding energy of hydrogen adatoms forming a dimer like structure, aside $B1$-$B2$, is higher than the binding energy of an isolated H_2 molecule. Since the formation of H dimer like structure may represents the initial stage of the hydrogen clustering process on graphene sheets, we can infer that the formation of H clusters are quite likely not only on the clean graphene sheets, which is in consonance with previous studies [Phys. Lett. **97**, 186102], but also on the $B1$-$B2$ boron doped graphene sheets. However, for low concentration of boron atoms, the formation of H dimer structures is not expected to occur nearby a single substitutional boron site. In this way, the formation (or not) of H clusters on graphene sheets can be tuned by the concentration of substitutional boron atoms.

PACS numbers: 73.20.Hb;73.20.-r

I. INTRODUCTION

Two dimensional crystals of sp^2 bonded carbon atoms, called graphene, exhibit quite different electronic and structural properties compared with their counterpart, *viz.*: graphite (graphene sheets stacked in ABABAB... arrangement), and carbon nanotubes (rolled up graphene sheets forming nanometer wide cylinders). Indeed, in a recent experimental study, Novoselov et al. [1] observed massless two dimensional (2D) Dirac fermions in free standing graphene sheets with high crystal quality. In this case, the electron scattering processes are suppressed, and thus, the charge carriers can propagate freely on the graphene surface. Meanwhile, very recently, Meyer at al. observed microscopic corrugations on a single layer suspended graphene sheet, due to the carbon atoms displaced out of the graphene plane. Such an experimental finding explain the thermodynamic stability of those isolated "two dimensional" systems, however, "further experimental and theoretical studies are needed to clarify the detailed mechanism of the corrugations in graphene" [2].

On graphene sheets, the sp^2 orbitals, forming σ bonding states parallel to the graphene surface, connect the carbon atoms arranged in a hexagonal lattice. While rise to delocalized π bonding and π^* anti-bonding states. The most of the electronic properties and the chemical reactivity of graphene sheets are ruled by those π and π^* orbitals. For instance, the already mentioned massless 2D Dirac fermions, and the recently observed control of the electronic properties in thin films composed by bilayer graphene sheets [3]. Focusing on the chemical properties, graphene has been considered as a candidate for hydrogen storage media [4, 5]. Scanning tunneling microscope (STM) pictures, of hydrogen adatoms on graphene surfaces, indicate a local electronic charge enhancement and long range electronic perturbation on the graphene sheet, giving rise to a local $(\sqrt{3}\times\sqrt{3})R30^o$ surface periodicity [6]. Hydrogen on graphene surface has been the subject of intense studies, not only addressing the realization of fuel cells based upon hydrogen storage, but also the formation of H_2 molecules in the interstellar medium (which is an important problem in astrophysics).

The energetic stability and the equilibrium geometry of hydrogen adatoms on graphene surfaces were investigated in detail by Sha and Jackson [7] and Duplock et al. [8]. They find binding energies of 0.67 and 0.76 eV/H atom, respectively, for a single hydrogen adatom chemisorbed on the graphene sheet. Having characterized the energetic and structural properties of hydrogen adatoms on graphene, further experi-

molecules through H–H recombination processes on the graphene surface. For instance, the Eley–Rideal reaction involving free hydrogen atoms (gas phase) and hydrogen adatoms chemisorbed on the graphene surface [7, 9]. On the other hand, the H–H recombination through hydrogen diffusion, on the graphene surface, represents another reaction path to obtain H_2 molecules from the chemisorbed hydrogen adatoms [10, 11, 12]. Based upon those H–H reaction processes, recent experimental studies, supported by *ab initio* calculations, examined the formation of hydrogen clusters on graphene surfaces [13]. Their findings suggest the formation of H dimer like structures as an initial stage of the observed hydrogen clusters chemisorbed on the graphene surface. The calculated binding energy of hydrogen adatoms forming a H dimer structure is higher compared with the binding energy of two isolated H monomers.

The binding energy of hydrogen adatoms chemisorbed on graphene sheets, as well as the formation of H clusters, can be tuned by suitable doping processes. For instance, the presence of substitutional boron atoms on graphene improve the hydrogen adsorption on the carbon atoms neighboring the boron substitutional sites [14, 15]. However, those calculated hydrogen binding energy results, as a function of substitutional boron concentration, are quite contradictory. Based upon Raman spectroscopy measurements, Endo et al. [16] characterized the equilibrium geometry of substitutional boron atoms on graphite. For boron concentration of ∼2.7% they find homogeneous distribution of substitutional boron atoms. Meanwhile, for higher concentration of substitutional boron atoms, about 17%, a detailed experimental study, performed by Hach et al. [17], indicates the formation of C_6B configuration. In the C_6B structure, the substitutional boron atoms occupy the opposite sites of a carbon hexagonal ring. Further experimental/theoretical studies have been done aiming to improve our knowledge related to boron doped graphite systems [18, 19, 20].

In the present paper we report an *ab initio* total energy investigation of boron doped graphene sheets, and the chemisorption processes of hydrogen adatoms as a function of boron concentration. The presence of substitutional boron atoms increases the electronic density of states near the Fermi level. Our calculated STM images indicate the formation of bright spots on the boron substitutional sites, which is in agreement with the experimentally obtained STM pictures [18]. For higher concentration of substitutional boron atoms, around 2.4%, we find that the two boron atoms lying on the opposite sites of the same hexagonal ring represents the energetically most stable structure. This geometry represents the building block of the C_6B structure [17]. The formation of H dimer like structure on graphene has been confirmed, as well as the increase of hydrogen binding energy nearby the boron substitutional sites. However, in contrast with the previous studies, here we have considered the most likely configuration for the substitutional boron atoms H dimer structure, neighboring a single boron substitutional site, is energetically less favorable compared with two isolated H monomers. Meanwhile, the formation of H dimer structure is expected for higher concentration of boron atoms, i.e., two substitutional boron atoms occupying the opposite sites of a hexagonal carbon ring, $B1$-$B2$. In this case, the binding energy of H adatoms is higher compared with the binding energy of an isolated H_2 molecule.

II. METHOD OF CALCULATIONS

Our calculations were performed in the framework of the spin polarized density functional theory (DFT) [21], within the generalized gradient approximation due to Perdew, Burke, and Ernzerhof [22]. The electron–ion interaction was treated by using norm–conserving, *ab initio*, fully separable pseudopotentials [23]. The Kohn–Sham wave functions were expanded in a combination of pseudoatomic numerical orbitals [24]. Double zeta basis set including polarization functions (DZP) was employed to describe the valence electrons [25]. The self–consistent total charge density was obtained by using the SIESTA code [26]. Graphene sheets were described within the supercell approach, by a single layer of graphene with 84 atoms, separated by 15 Å from their image. A mesh cutoff of 170 Ry was used for the reciprocal–space expansion of the total charge density, and the Brillouin zone was sampled by using up to 15 special **k** points. We have verified the convergence of our results with respect to the number and choice of the special **k** points. All atoms of graphene sheets were fully relaxed within a force convergence criterion of 20 meV/Å.

III. RESULTS AND COMMENTS

A. Boron

Initially we examined the equilibrium geometry and the electronic properties of boron doped graphene sheet. For a single substitutional boron atom, $B1$ in Fig. 1(a), we obtained a B–C bond length (d_{B-C}) of 1.50 Å, while the nearest neighbor C–C bonds are slightly compressed (by ∼0.01 Å) compared with the undoped system. The structural deformations of graphene are very localized around the substitutional boron site. Experimental STM measurements indicate d_{B-C} of 1.59 Å [19] which is in agreement with our calculated results.

Graphene sheets are metallic, as indicated by density of states (DOS) diagrams shown in Figs. 2(a) and 2(d), dashed lines. Such a metallic character has been kept for boron doped graphene (solid lines), however, the electronic density of states near the valence band maximum increases compared with the pristine system (shaded regions). Figure 2(b) presents the localization of the elec-

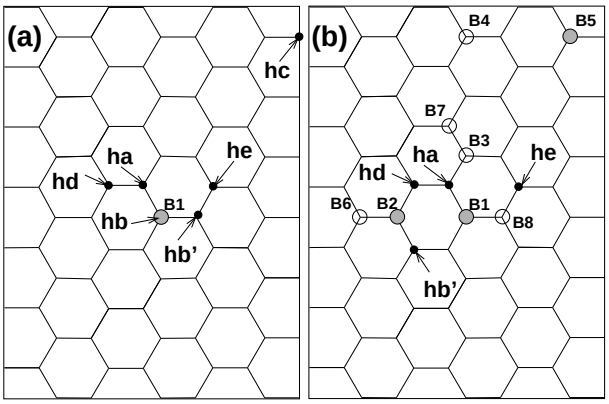

FIG. 1: Structural models of boron doped graphene sheet for, (a) a single substitutional boron atom ($B1$), and (b) two substitutional boron atoms per unit cell ($B1-B2$), corresponding to boron concentrations of ∼1.2 and 2.4 %, respectively.

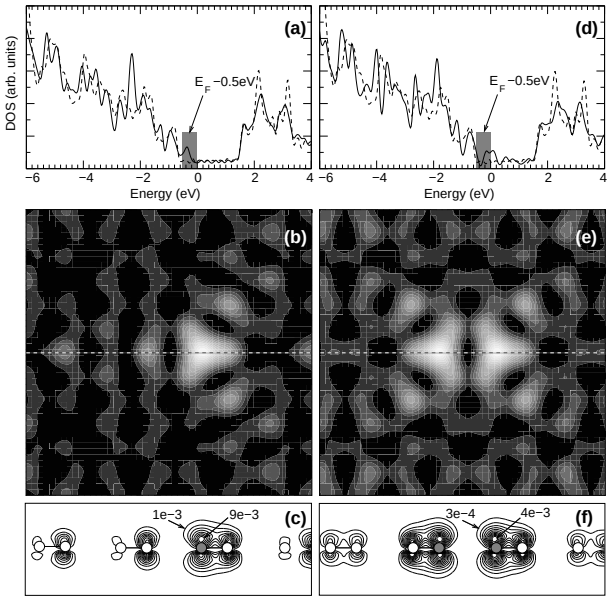

FIG. 2: Calculated density of states (a)/(d), STM images for occupied states within an energy interval of 0.5 eV below the Fermi level (b)/(e), and electronic distribution of the highest occupied states ($E_F - 0.5$ eV) along the C–B bonds (c)/(f) (unit: e/bohr^3), for the structural models $B1$/$B1$-$B2$.

the Fermi level ($E_F - 0.5$ eV). In this diagram, the higher lying occupied states are projected onto a parallel plane at 1.25 Å from the graphene sheet. Within the Tersoff–Hamman approach [27], this projected local density of states [Fig. 2(b)] corresponds to the STM images of boron–doped graphene sheet. The bright protrusion on the substitutional boron (center) and the nearest neighbor carbon atoms (edges) indicate that the occupied electronic states, within $E_F - 0.5$ eV, are concentrated around the boron substitutional site. Those bright spots come from π bonding states of $2p_z$ orbitals along the B–C bonds, see Fig. 2(c). The formation of bright regions around the substitutional B atoms is in accordance with the experimentally obtained STM pictures [19].

Within our supercell approach, a single substitutional boron atom corresponds to a boron concentration of ∼1.2 %. Two boron atoms per supercell corresponds to a boron concentration of ∼2.4 %. In this case, we have considered several plausible Bi-Bj configurations, indicated in Fig. 1(b), for boron atoms occupying substitutional sites on graphene sheet. Our total energy results, summarized in Table I, reveal the formation of preferential domains, or preferential configurations for substitutional boron atoms on graphene, *viz.*: two boron atoms occupying the opposite sites of the same hexagonal ring, $B1$-$B2$ in Fig. 1(b), represents the energetically most stable configuration. Whereas $B1$-$B8$ is the energetically least favorable structure. The former geometry, $B1$-$B2$, was proposed by Hach et al. for "boron rich carbon structures" [17]. The structural models $B1$-$B4$ and $B1$-$B5$ are slightly less favorable compared with $B1$-$B2$. Since in $B1$-$B4$ and $B1$-$B5$ the boron atoms are placed far from each other, d(B–B) = 7.5 and 8.6 Å, respectively. We can infer that at low concentration regime, the substitutional boron atoms may spread out the graphene sheet. Whereas, under B-rich condition the formation of $B1$-$B2$ becomes dominant, giving rise to C_6B like structures [17]. In both $B1$-$B2$ arrangements the building block

TABLE I: Total energy differences, ΔE (eV/B atom), and B–B distances in Å.

Configuration	ΔE	d(B–B)
$B1$-$B2$	0.00	2.87
$B1$-$B3$	0.17	2.53
$B1$-$B4$	0.02	7.49
$B1$-$B5$	0.01	8.64
$B1$-$B6$	0.08	4.33
$B1$-$B7$	0.12	3.86
$B1$-$B8$	0.66	1.58

of the proposed C_6B structure.

Figure 2(d) (solid line) presents our calculated DOS for the structural model $B1$-$B2$. We observe that the electronic density of states increases near valence band maximum (shaded region) compared with the undoped system (dashed line). The occupied electronic states within $E_F - 0.5$ eV are mainly localized on the substitutional boron and neighboring the carbon atoms, giving rise to the two bright protrusions shown in Fig. 2(e). Figure 2(f) indicates that such a STM picture originates from the π orbitals along the B–C bonds.

It is worth to pointing out that the unlikely $B1$-$B3$ and $B1$-$B7$ [15] and $B1$-$B8$ [14] arrangements (ΔE = 0.17, 0.12, and 0.66 eV/B atom, respectively) were considered as substrates for hydrogen adsorption on boron doped graphene. Thus, we believe that further studies are necessary addressing the role played by substitutional boron impurities for hydrogen adsorption processes, now con-

the substitutional boron atoms, $B1$-$B2$.

B. Hydrogen

Having established the energetically most probable structures for substitutional boron atoms on graphene, *viz.*: structural models $B1$ [Fig. 1(a)] and $B1$-$B2$ [Fig. 1(b)], in this section we examined the hydrogen adsorption processes on the clean and boron doped graphene sheets.

Firstly, using the 84-atoms unit cell [Fig. 1(a)], we calculate the binding energy of hydrogen adatoms on clean graphene. For a single hydrogen adatom we find a binding energy (E^b_H) of 0.98 eV/H-atom. The C–H equilibrium bond length is 1.14 Å, which indicates the formation of a C–H covalent bond, while the carbon atom underneath the hydrogen adatom moves upward by 0.5 Å from the flat graphene layer. For an isolated hydrogen molecule, we calculate a binding energy of 4.34 eV/H_2-molecule (2.17 eV/H-atom). Thus, with respect to the H_2 molecule, the hydrogen adsorption on graphene is an endothermic process by 1.19 eV/H-atom. Our total energy and equilibrium geometry results are in agreement with previous *ab initio* studies of hydrogen adsorption on the graphene sheet, for instance, E^b_H of 0.7–0.8 eV/H-atom and C–H bond length of 1.13 Å [7, 8, 13].

In a very recent study, Hornekær et al. observed that the presence of a hydrogen adatom on graphene surface gives rise to preferential adsorption sites (nearby the already adsorbed hydrogen adatom) for the subsequent hydrogen sticking process [13]. Indeed we find that a hydrogen adatom lying on ha increases the binding energy of the next hydrogen adatom (E^b_{HH}) on hd or he [cf. Fig. 1(a)]. We calculate $E^b_{HH} = 2.03$ eV/H-atom for both hydrogen configurations, ha/hd and ha/he, while Hornekær et al. obtained binding energies of 1.9 and 2.1 eV/H-atom, respectively. Those results indicate that the formation of ha/hd or ha/he hydrogen dimer like structures are energetically more favorable compared with two isolated ha monomers, that is, $ha{+}ha \rightarrow ha/hd$, ha/he are exothermic processes. Our findings are in accordance with previous studies related to the formation of hydrogen clusters on graphene surface. In addition, our calculated binding energies E^b_{HH} (for ha/hd and ha/he) are comparable with the binding energy of an isolated H_2 molecule (2.17 eV/H-atom). Suggesting that presence of a single hydrogen adatom (ha) on the graphene sheet, somewhat promote the H_2 dissociation nearby ha.

The binding energy of a single hydrogen adatom, E^b_H, increases upon the presence of substitutional boron atoms on the graphene surface. Our results of binding energies are summarized in Table II. For the $ha/B1$ configuration, depicted in Fig. 3(a), we find $E^b_H = 1.89$ eV/H-atom, whereas on the clean graphene surface we have $E^b_H = 0.98$ eV/H-atom. So that, we can infer that presence of a substitutional boron atom, in the vicin-

TABLE II: Binding energies (E^b) of hydrogen adatoms on clean and boron doped graphene surface in eV/H-atom.

Model	E^b_H		E^b_{HH}				
	ha	hb	ha/hb	ha/hb'	ha/hc	ha/hd	ha/he
clean	0.98	–	–	–	–	2.03	2.03
$B1$	1.89	1.51	1.36	1.51	1.00	1.67	1.25
$B1$-$B2$	2.13	–	–	1.73	–	2.37	1.64

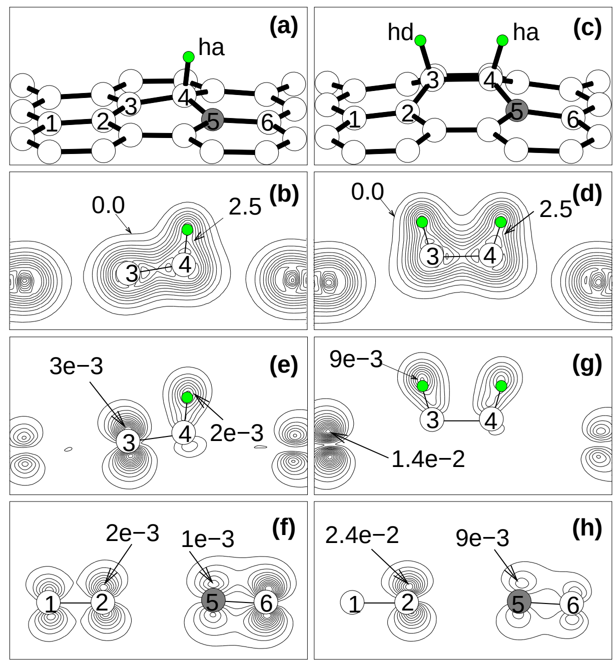

FIG. 3: Equilibrium geometry and total charge density of hydrogen adatoms on the $B1$ graphene sheet, (a)–(b) ha and (c)–(d) ha/hd models. Partial electronic charge density within $E_F - 0.5$ eV for (e)–(f) ha and (g)–(h) ha/hd models. Unit, e/bohr^3.

H bond by 0.91 eV. Meanwhile, the hydrogen adsorption on top of the substitutional boron atom, $hb/B1$, is energetically less favorable by 0.38 eV/H-atom compared with $ha/B1$. At the equilibrium geometry, the C–H bond length is 1.15 Å and the C atom (underneath the hydrogen adatom) moves upward by 0.4 Å. The formation of C–H covalent bond is depicted in Fig. 3(b). Figures 3(e) and 3(f) present the occupied electronic states along the C–H and B–C bonds, respectively, within $E_F - 0.5$ eV . Those electronic states are composed by π orbitals of carbon and (substitutional) boron atoms on the graphene sheet, and sp_z σ hybridization along the C–H bond [Fig. 3(e)]. Comparing the electronic densities depicted in Figs. 2(c) and 3(f), $B1$ and $ha/B1$ structures, respectively, we can infer that the hydrogen adsorption on ha reduces the electronic density of occupied π orbitals along the B–C bonds.

Keeping the $B1$ configuration adsorbed by a hydrogen adatom ($ha/B1$), the subsequent hydrogen adsorp-

plausible configuration for two hydrogen adatoms on $B1$ graphene sheet. Our binding energy results for the hydrogen adatom on the $ha/B1$ graphene sheet, E^b_{HH}, indicate that ha/hc represents the energetically least stable configuration. We find E^b_{HH} = 1.00 eV/H-atom, nearly the same hydrogen binding energy on the clean graphene, E^b_H = 0.98 eV/H-atom. This result is somewhat expected, since hc is far from the substitutional boron site, $B1$. Figure 3(c) presents the energetically most stable configuration, ha/hd, E^b_{HH} = 1.67 eV/H-atom. The C–H bond length is equal to 1.14 Å, and its covalent character is depicted in Fig. 3(d). Similar to the $ha/B1$ system, the electronic states within $E_F - 0.5$ eV are composed by sp_z σ hybridization along the C–H bonds, and π orbitals of carbon and boron atoms, Figs. 3(g) and 3(h), respectively. However, in this case, the adsorption of the second hydrogen adatom (hd) is not favored by the presence of the first one (ha), E^b_{HH} is lower than E^b_H. Consequently, ha+$ha \rightarrow ha/hd$ is an endothermic process, thus, indicating that the formation of hydrogen clusters is not expected to occur nearby single boron substitutional sites. Thus, for higher coverage of hydrogen adatoms, we can infer that hydrogen clusters on the clean region graphene surface, i.e. far from boron substitutional sites (with $E^b_{HH} \approx 2.0$ eV/H-atom) are more likely than hydrogen adatoms neighboring an isolated boron substitutional site ($E^b_{HH} \approx 1.7$ eV/H-atom).

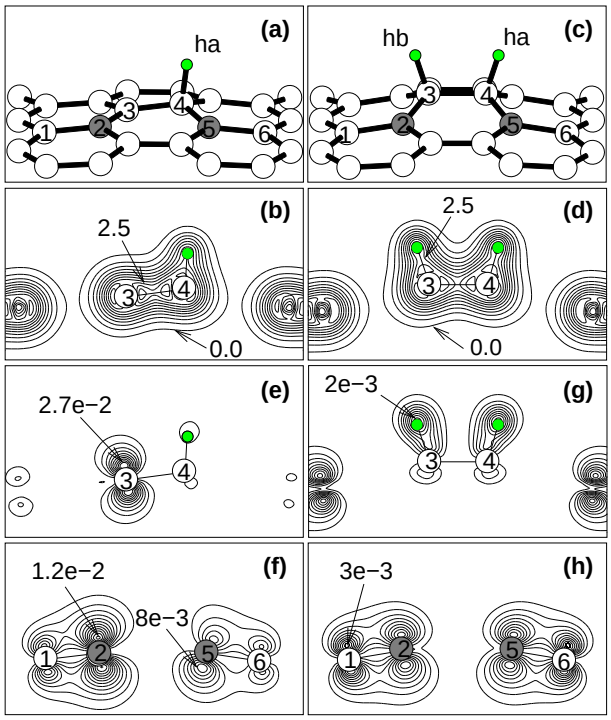

FIG. 4: Equilibrium geometry and total charge density of hydrogen adatoms on the $B1$-$B2$ graphene sheet, (a)–(b) ha and (c)–(d) ha/hd models. Partial electronic charge density within $E_F - 0.5$ eV for (e)–(f) ha and (g)–(h) ha/hb models. Unit, e/bohr^3.

Increasing the concentration of substitutional boron atoms, forming the energetically most probable configuration, i.e. $B1$-$B2$ [Fig. 1(b)], the binding energy of hydrogen adatoms increases compared with the $B1$ graphene surface. For a single hydrogen adatom, $ha/B1$-$B2$ in Fig. 4(a), we find E^b_H equal to 2.13 eV/H-atom, which is comparable with the calculated H_2 binding energy (2.17 eV/H-atom). At the equilibrium geometry, the C–H bond length is 1.15 Å, and the formation of C–H covalent bond is depicted in Fig. 4(b). Figure 4(e) shows that the sp_z σ orbitals does not lie within $E_F - 0.5$ eV. Whereas the p_z orbital of the carbon atom C(3) strongly contributes to the electronic states within this energy interval. The former σ bonding states, composed by hydrogen s and carbon p_z orbitals, are resonant within the valence band of the graphene sheet. In addition, comparing 2(f) and 4(f) we verify that electronic density of π orbitals along the B–C bonds increases (asymmetrically) upon hydrogen adsorption.

Different from ha/hd on the $B1$ graphene sheet, the formation of ha/hd dimer like structure on $B1$-$B2$, namely ha+$ha \rightarrow ha/hd$, is an exothermic process by 0.24 eV/H-atom. Furthermore, E^b_{HH} is higher than the binding energy of H_2 molecule, that is, the formation of ha/hd on the boron doped $B1$-$B2$ graphene surface is an exothermic process by 0.20 eV/H-atom compared with free H_2 molecules. Thus, we can infer that the formation of hydrogen clusters can be improved by the increase of substitutional boron atoms forming the C_6B like structure on the graphene surface. Figure 4(d) presents the total charge density along the C–H covalent bonds. The carbon atoms bonded to hydrogen adatoms exhibit sp^3 like hybridizations, where C(3) and C(4) are displaced upward by 0.94 Å with respect to the pristine graphene sheet. The C(3)–C(4) equilibrium bond length (1.54 Å) is stretched by 0.1 Å compared with the C–C bond length of undoped systems. The localization of the occupied electronic states, within $E_F - 0.5$ eV, are depicted in Figs. 4(g) and 4(h). In the latter diagram we find that the electronic density of the π orbitals along the B–C bonds is reduced compared with the π orbitals of $ha/B1$ [Fig. 4(f)]. Figure 4(g) depicts the sp_z σ orbitals along the C–H bonds. In a STM measurement, those sp_z states will give rise to bright spots on the hydrogen adatoms lying on the $B1$-$B2$ boron doped graphene sheets. Indeed, recent STM pictures, supported by *ab initio* simulations, indicate the formation of bright protrusions attributed to the hydrogen adatoms (forming a dimer like structure) on clean graphene sheets [11]. On the other hand, quite different STM pictures are expected for $ha/B1$-$B2$. Figure 4(e) indicates that, for STM bias voltage of ∼0.5 V below the Fermi level, the tunneling current from the hydrogen adatoms will be negligible compared with the one from neighbor carbon and boron atoms. Thus, in this case, the hydrogen adatom site will appear darker than

IV. CONCLUSIONS

In summary, we have performed an *ab initio* total energy investigation of boron doped graphene sheets, and their interaction with hydrogen adatoms. For a single substitutional boron atom, the equilibrium geometry of graphene sheet is weakly perturbed, while the electronic density of states near the valence band maximum has been increased. Our simulated STM images indicate the formation of bright (triangular) spots on the boron substitutional site (center) and the nearest neighbor carbon atoms (edges). For two boron atoms occupying the substitutional sites on the graphene sheet, corresponding to a boron concentration of ∼2.4%, we find that boron atoms lying on the opposite sites of the same hexagonal ring ($B1$-$B2$ structure) represents the energetically most stable configuration. Furthermore, the hydrogen adsorption on graphene has been examined as a function of the concentration of boron atoms. For the pristine graphene system, we find that the binding energy of hydrogen adatoms forming H dimer like configurations (ha/hd or ha/he) is higher by 1 eV/H-atom compared with the binding energy of two isolated H monomers (E_H^b = 0.98 eV/H-atom). This is in accordance with the recent experimental/theoretical study of the formation of H clusters on graphene sheets [11, 13]. The presence of a single substitutional boron atom increases the hydrogen binding energy by 0.9 eV/H-atom compared with the one on the clean graphene sheet. In this case, the hydrogen adatom lies on top of the carbon atom nearest neighbor to the substitutional B site ($ha/B1$ configuration). However, different from the pristine system, the adsorption of two hydrogen adatoms close to each other, forming a H dimer like structure, is energetically less favorable compared with two isolated H monomers. This result indicates that the formation of hydrogen clusters on the graphene sheet is somewhat suppressed by the presence of a single substitutional boron atom. Finally, for boron concentration of ∼2.4% we find that the binding energy of H dimer structure (E_{HH}^b) is higher than the binding energy of an isolated H_2 molecule, where the hydrogen adatoms lie on the carbon atoms neighboring the substitutional boron sites. In this case, boron atoms give rise to preferential adsorption sites for hydrogen adatoms on graphene sheets, and thus, improving the formation of hydrogen clusters on graphene sheets. Those results indicate that the formation (or not) of H clusters on graphene sheets can be tuned by the concentration of substitutional boron atoms.

Acknowledgements

The authors acknowledge financial support from the Brazilian agencies CNPq, FAPEMIG, and FAPESP, and the computational facilities of the Centro Nacional de Processamento de Alto Desempenho/CENAPAD-Campinas.

[1] K. S. Novoselov, A. K. Geim, S. V. Morozov, D. Jiang, M. I. Katsnelson, V. Grigoreva, S. V. Dubonos, and A. A. Firsov, Nature **438**, 197 (2005).
[2] J. C. Meyer, A. K. Geim, M. I. Katsnelson, K. S. Novoselov, T. J. Booth, and S. Roth, Nature **446**, 60 (2007).
[3] T. Ohta, A. Bostwick, T. Seyller, K. Horn, and E. Rotenberg, Science **313**, 951 (2006).
[4] L. Schlapbach and A. Züttel, Nature **414**, 353 (2001).
[5] S. Patchkovskii, J. S. Tse, S. N. Yurchenko, L. Zhechkov, T. Heine, and G. Seifert, Proc. Natl. Acad. Sci. USA **102**, 10439 (2005).
[6] P. Ruffieux, O. Gröning, P. Schwaller, L. Schlapbach, and P. Gröning, Phys. Rev. Lett. **84**, 4910 (2000).
[7] X. Sha and B. Jackson, Surf. Sci. **496**, 318 (2002).
[8] E. J. Duplock, M. Scheffler, and P. J. D. Lindan, Phys. Rev. Lett. **92**, 225502 (2004).
[9] X. Sha, B. Jackson, and D. Lemoine, J. Chem Phys. **116**, 7158 (2002).
[10] Y. Ferro, F. Marinelli, A. Allouche, and C. Brosset, Chem. Phys. Lett. **368**, 609 (2003).
[11] L. Hornekær, Ž. Šljivančan, W. Xu, R. Otero, E. Rauls, I. Stensgaard, L. Lægsgaard, and F. Besenbacher, Phys. Rev. Lett. **96**, 156104 (2006).
[12] S. Baouche, G. Gamborg, V. V. Petrunin, A. C. Luntz, A. Baurichter, and L. Hornekær, The J. Chem. Phys. **125**, 084712 (2006).
[13] L. Hornekær, E. Rauls, W. Xu, Ž. Šljivančanin, R. Otero, I. Stensgaard, and L. Lægsgaard, Phys. Rev. Lett. **97**, 186102 (2006).
[14] Y. Ferro, F. Marinelli, A. Allouche, and C. Brosset, J. Chem. Phys. **118**, 5650 (2003).
[15] Z. Zhu, G. Lu, and H. Hatori, J. Chem. Phys. B **110**, 1249 (2006).
[16] M. Endo, C. Kim, T. Karaki, T. T, Y. Nishumura, M. J. Matthews, S. D. M. Brown, and M. Dresselhaus, Phys. Rev. B **58**, 8991 (1998).
[17] C. T. Hach, L. E. Jones, C. Crossland, and P. A. Thrower, Carbon **37**, 221 (1999).
[18] M. Endo, C. Kim, T. Karaki, Y. Nishumura, M. J. Matthews, S. D. M. Brown, and M. Dresselhaus, Carbon **37**, 561 (1999).
[19] M. Endo, T. Hayashi, Seong-Hwa-Hong, T. Enoki, and M. Dresselhaus, J. Appl. Phys. **90**, 5670 (2001).
[20] I. Suarez-Martinez, A. A. El-Barbary, G. Savini, and M. I. Heggie, Phys. Rev. Lett. **98**, 015501 (2007).
[21] P. Hohenberg and W. Kohn, Phys. Rev. **136**, B864 (1964).
[22] J. P. Perdew, K. Burke, and M. Ernzerhof, Phys. Rev. Lett. **77**, 3865 (1996).
[23] L. Kleinman and D. M. Bylander, Phys. Rev. Lett. **48**, 1425 (1982).
[24] O. F. Sankey and D. J. Niklewski, Phys. Rev. B **40**, 3979 (1989).
[25] E. Artacho, D. Sánchez-Portal, P. Ordejón, A. Garcia,

[26] J. M. Soler, E. Artacho, J. D. Gale, A. García, J. Junquera, P. Ordejón, and D. Sánchez-Portal, J. Phys.: Condens. Matter **14**, 2745 (2002).

[27] J. Tersoff and D. R. Hamann, Phys. Rev. B **31**, 805 (1985).